31st Annual International Conference of the IEEE EMBS
Minneapolis, Minnesota, USA, September 2-6, 2009

L1-norm and L2-norm Neuroimaging Methods in Reconstructing Extended Cortical Sources from EEG

Lei Ding *Member, IEEE*
University of Oklahoma, Norman, Oklahoma

Abstract- **We have previously reported a new sparse neuroimaging method (i.e. VB-SCCD) using the L1-norm optimization technology to solve EEG inverse problems. The new method distinguishes itself from other reported L1-norm methods since it explores the sparseness in a transform domain rather than in the original source domain. In the present study, we conducted a Monte Carlo simulation study to compare the performance of VB-SCCD and other two popular L2-norm neuroimaging methods (i.e. wMNE and cLORETA) in reconstructing extended cortical neural electrical activations. Our simulation data suggests that the VB-SCCD method is able to reconstruct extended cortical sources with the overall high accuracy. It has significantly higher accuracy, less number of false alarms and less number of missing sources when studying complex brain activations (up to 5 simultaneous sources). This new sparse neuroimaging method is thus promising to have many valuable applications in neuroscience and neurology problems. It is also applicable to MEG neuroimaging.**

Keywords- **sparse neuroimaging, sparseness, regularization, L1-norm, transform domain, EEG, SCOP**

I. Introduction

Mathematically, EEG inverse problems, which attempt to localize brain electrical activations from scalp measurable electrical signals (i.e. EEG), have no unique solutions and are highly ill-posed [1, 2]. Historically, favorable EEG inverse solutions in various conditions have been obtained by implementing different neural source models [2]. Among these neural source models, the cortical current density (CCD) source model [3] has been implemented through the segmentation of structural brain data from magnetic resonance imaging (MRI), and is widely used to study important problems in neuroscience and clinical neurology.

The forward relationship between sources defined on the CCD model and EEG measurements can be described by a set of linear equations. This set of equations is highly underdetermined and its inverse solution is extremely sensitive to noise, which reflects the general characteristics of EEG inverse problems, i.e. non-uniqueness and ill-conditioning. These linear equations are usually solved through regularization schemes, such as in the minimum norm estimate (MNE) method, which selects the current distribution that explains the measured data with the smallest Euclidean norm (L2-norm) of the current sources [4], and its variants [5-8]. Generally, L2-norm based MNE methods can explicitly formulate the process to obtain inverse solutions as linear operators, which significantly reduces the computational needs. However, L2-norm MNE methods suffer significantly from their low spatial resolutions [8, 9]. In order to reconstruct sparse and compact neural sources, L1-norm based MNE methods have been explored [10-13]. While L2-norm MNE methods produce over-smooth inverse solutions, L1-norm MNE methods, as those reported in literatures [10-13], produce over-focused inverse solutions, which usually only involves activations from a single element on the CCD model. Thus both L1- and L2-norm MNE methods have their limitations in reconstructing spatially extended cortical sources and estimating their extents on the cortical surface.

Recently, we have reported a new L1-norm neuroimaging method [9], i.e. the variation-based sparse cortical current density (VB-SCCD) method. In principle, the VB-SCCD method is distinguished from MNE methods, which utilizes the concept of sparse neuroimaging. The objective functions in sparse neuroimaging are defined to represent cortical current density distribution with minimal non-zero coefficients (sparseness). The variation map of cortical current densities is used in VS-SCCD to characterize the sparseness on boundaries between active cortical regions (sources) and inactive cortical regions (no sources). The L1-norm optimization algorithm is then used to reconstruct these non-zero coefficients in variation maps and, thus, to recover cortical current density distributions.

In the present work we conducted a comparison study between two L2-norm methods (i.e. weighted MNE (wMNE) [7] and cortical low resolution electromagnetic tomography (cLORETA)) and the L1-norm VB-SCCD method. Their performance in reconstructing extended cortical sources was evaluated using metrics, i.e. receiver operation curve (ROC) and area under curve (AUC), from the detection theory [15], with randomly simulated extended cortical sources (i.e. Monte Carlo study [16]). We studied conditions with 1, 2, and 5 randomly located cortical sources with high-density EEG measurements (i.e. 120 channels). Our present results show the performance of VB-SCCD is significantly better than wMNE and cLORETA in reconstructing extended cortical sources. Previously reported other L1-norm MNE methods were not considered in this comparison study since their solutions are over-focused and not suitable to recover extents of spatially distributed sources.

II. Method

A. L2-norm and L1-norm Neuroimaging Methods

The regularization scheme used in wMNE can be expressed as

$$\min\left\|W\bar{s}\right\|_2 \qquad subject\ \ to\ \ \left\|\bar{\phi}-A\bar{s}\right\|_2<\beta \qquad (1)$$

where β is the regularization parameter. Here, W is an

$N \times N$ diagonal matrix with each diagonal element defined as $W_{ii} = \sqrt{A_i^T A_i}$ to compensate the bias due to the source depth [5]. The cLORETA method [14] can be expressed as

$$\min \left\| LW\bar{s} \right\|_2 \qquad subject \quad to \quad \left\| \bar{\phi} - A\bar{s} \right\|_2 < \beta \qquad (2)$$

Here, L is the two-dimensional discrete spatial Laplacian operator defined over the cortical surface. By minimizing the high spatial frequency components, cLORETA maximizes the chance to produce smooth source reconstructions.

The new sparse neuroimaging method (i.e. VB-SCCD) explores the sparseness in the transform domain (i.e. the variation map), instead of the original source domain, which can only produce over-focused EEG inverse solutions [10-13]. The regularization scheme in VB-SCCD could be mathematically expressed as

$$\min \left\| V\bar{s} \right\|_1 \qquad subject \quad to \quad \left\| \bar{\phi} - A\bar{s} \right\|_2 < \beta \qquad (3)$$

where V is a matrix operator to get the variation map of cortical current density distributions. The variation vector is thus defined as $V\bar{s}$. Each element in this variation vector represents a coefficient within the variation map over a triangular edge in the CCD model and its value indicates the current density difference between two triangular elements sharing the same edge (see [9] for details). If the cortical current density within each active cortical source is close to uniform or can be approximated with uniform distributions, non-zero coefficients are expected to largely happen on boundaries (the sparseness), and can be identified by minimizing the L1-norm of current density variation maps.

The regularization parameter β in equations (1), (2), and (3) can be estimated by applying the discrepancy principle [17]. We choose it high enough so that the probability of $\left\| \bar{n} \right\|_2 \geq \beta$, where $\bar{n} = \bar{\phi} - A\bar{s}$, is small. When noises are Gaussian white, $\left(1/\sigma^2\right)\left\| \bar{n} \right\|_2^2$, where σ^2 denotes the variance, has the χ_m distribution with M degrees of freedom, i.e. $\left(1/\sigma^2\right)\left\| \bar{n} \right\|_2^2 \sim \chi_m^2$. In practice, the upper bound of $\left\| \bar{n} \right\|_2$, i.e. β, is selected such that the confidence interval $[0, \beta]$ integrates to a 0.99 probability [13]. While the GWN is not a good approximation of real noise, other noise models can be similarly utilized if the distributions of noise are known or can be estimated.

B. Solvers for wMNE, cLORETA and VB-SCCD

The optimization problems stated in equations (1)-(3) belong to the convex optimization problems, which were solved by the second order cone programming (SOCP) technique [18]. The SOCP has efficient globally convergent solver known as the Interior Point Methods (IPM). The IPM method has been implemented in a MATLAB package named SeDuMi [19]. In order to be solved, every problem must be formatted into the framework of SOCP below in either the primal form or the dual form:

$$\begin{aligned} &\min \quad \bar{c}^T \bar{x} \\ &subject \quad to \quad B\bar{x} = \bar{b} \\ &\quad \bar{x} \in Lorentz \quad cone \end{aligned} \qquad \text{or}$$

$$\begin{aligned} &\max \quad \bar{b}^T \bar{x} \\ &subject \quad to \quad \bar{c} - B^T \bar{x} \in Lorentz \quad cone \end{aligned} \qquad (4)$$

$$Lorentz \quad cone := \left\{ (u_1, u_2, \ldots, u_p) \in R \times R^{n-1} \left| u_i \right| \geq \left\| u_1, \ldots, u_j, \ldots u_p \right\|_2 \quad j \neq i \right\}$$

where $\bar{x} = \left[x_1, x_2, \ldots, x_p \right]^T$ is the solution vector for a SOCP problem (not the source vector $\bar{s}$). $\bar{b}$ and $\bar{c}$ are the coefficient vectors and B is the coefficient matrix, which were defined specifically in each given problem. Here, we used the dual form to convert (1)-(3) into (5)-(6) for wMNE, cLORETA, and VB-SCCD, respectively, by introducing certain intermediate variables:

$$\max \quad \bar{b}^T \bar{x} = -\begin{bmatrix} \bar{0}^T & \bar{0}^T & \bar{0}^T & 1 \end{bmatrix} \begin{bmatrix} \bar{s} \\ \bar{h} \\ \bar{z} \\ t \end{bmatrix} \qquad \begin{array}{l} subject \quad to \quad \bar{z} = \bar{\phi} - A\bar{s} \\ \left\| \bar{z} \right\|_2 \leq \beta \\ W_{i,*}\bar{s} = h_i \quad i = 1,2,\cdots,N \\ \left\| h_1, \ldots, h_i, \ldots, h_N \right\|_2 \leq t \end{array} \qquad (5)$$

$$\max \quad \bar{b}^T \bar{x} = -\begin{bmatrix} \bar{0}^T & \bar{0}^T & \bar{0}^T & 1 \end{bmatrix} \begin{bmatrix} \bar{s} \\ \bar{h} \\ \bar{z} \\ t \end{bmatrix} \qquad \begin{array}{l} subject \quad to \quad \bar{z} = \bar{\phi} - A\bar{s} \\ \left\| \bar{z} \right\|_2 \leq \beta \\ L_{i,*}W\bar{s} = h_i \quad i = 1,2,\cdots,N \\ \left\| h_1, \ldots, h_i, \ldots, h_N \right\|_2 \leq t \end{array} \qquad (6)$$

$$\max \quad \bar{b}^T \bar{x} = -\begin{bmatrix} \bar{0}^T & \bar{0}^T & \bar{0}^T & \bar{1}^T \end{bmatrix} \begin{bmatrix} \bar{s} \\ \bar{h} \\ \bar{z} \\ \bar{t} \end{bmatrix} \qquad \begin{array}{l} subject \quad to \quad \bar{z} = \bar{\phi} - A\bar{s} \\ \left\| \bar{z} \right\|_2 \leq \beta \\ V_{i,*}\bar{s} = h_i \quad i = 1,2,\cdots,P \\ \left\| h_i \right\|_2 \leq t_i \quad i = 1,2,\cdots,P \end{array} \qquad (7)$$

Here the coefficient vector $\bar{b}$ and the solution vector $\bar{x}$ have been explicitly defined by relating to the source vector $\bar{s}$ and introduced intermediate variables $\bar{z}$, $\bar{h}$, and t in (5) and (6) or $\bar{t}$ in (7). The vector $\bar{c}$ and the matrix B in (4) could be explicitly expressed by reformatting the nonlinear constraints on the measurement errors, i.e. $\left\| \bar{z} \right\|_2 \leq \beta$, and those related to $\bar{h}$. SeDuMi also introduces so-called free variables [19], which are not in the standard dual form of a SOCP problem, to handle linear constraints in (5)-(7) and all of these linear constraints are formatted into $\bar{c}_l - B_l^T \bar{x} = \bar{0}$ (the subscript l here indicates coefficients in the vector and matrix for linear constraints). The intermediate variable t in (5) and (6) is a scalar representing the weighted L2-norm of vectors. Each element of the vector $\bar{t}$ in (7) represents the absolute difference of current densities at a pair of neighboring elements, where $V_{i,*}$ is ith row of V in (3). Since the size of these optimization problems is large (over 60000 elements in the source space as discussed below), the computational time for each problem discussion in (5)-(7) ranges from about half minutes to about fifteen minutes (depending on the number of simulated sources).

C. Simulation Protocol

The cortical surface was triangulated into a high-resolution mesh with a total of 67864 triangles (triangle area: 3.52 ± 1.47 mm^2 (mean ± SD)) to build the CCD model. Cortical sources were generated by selecting a seed triangular voxel on the cortical mesh and gradually growing into patches by iteratively adding neighboring elements. The dipole moment on each triangle was computed as the multiplication of the individual triangular area and the dipole moment density (assume 100 pAm/mm^2). Different brain

activations were simulated with different number of cortical sources (i.e. 1, 2, and 5 simultaneous sources). The locations of sources in these brain activations were randomly selected. The cortical extents of these sources ranged between 3 cm^2 to 5 cm^2, which was a relatively narrow range in order to keep sensitivity of EEG electrodes to every source at the similar level. For each condition (with different number of sources), we repeated 200 times in order to cover most parts of the brain during the random procedure.

Simulations were conducted in a three-shell boundary element (BE) model which simulated the three major tissues (the scalp, skull, and brain) with different conductivity values (0.33/Ω.m, 0.0165/Ω.m, and 0.33/Ω.m, respectively) [20]. We used the metrics, i.e. the receiver operating characteristic (ROC) curve and the area under the ROC curve (AUC) from the detection theory (see [9] for details) to evaluate the performance of neuroimaging methods. High AUC values indicate both high sensitivity and high specificity in reconstructing extended cortical sources.

III. Results

Fig. 1 summarizes the results, using Whisker plots, obtained from wMNE, cLORETA, and VB-SCCD during the Monte Carlo simulation as discussed above. Among all three methods, VB-SCCD has the highest AUC values in every simulated condition (i.e. 1, 2, or 5 sources). Even when there are 5 simultaneous sources, its median AUC value is still close to 0.8, which is believed of high accuracy

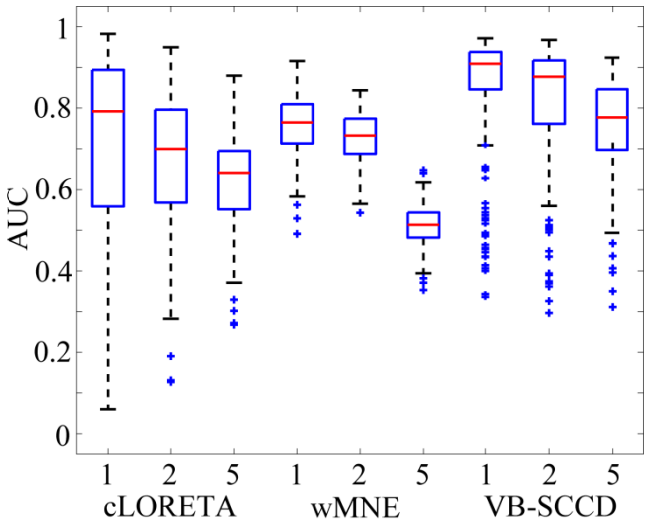

Figure 1 AUC metrics of 200 repeats (Whisker plots) for wMNE, cLORETA, VB-SCCD at different number of neural sources (i.e. 1 source, 2 sources, and 5 sources).

[15]. The wMNE method has the smallest variance on AUC values from 200 repeats, which is possibly because it has low AUC values in most of cases. On the other hand, the cLORETA method shows the largest variance on AUC values, especially at the condition of 1 source. This data indicates that the performance of cLORETA is highly dependent on source locations. It is worth to note that there are more outliers in the Whisker plots for VB-SCCD. This is a good indicator since the variance of AUC values from VB-

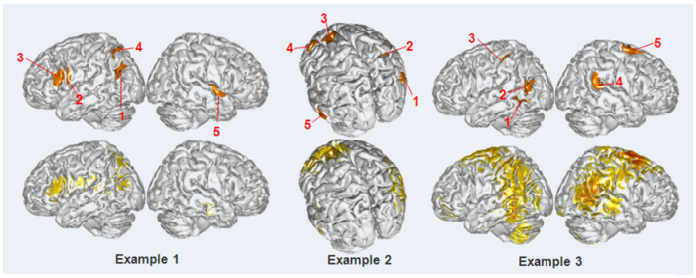

Figure 2 Visualization of three examples with the highest AUC values in the conditions of 5 simultaneous brain activations from the wMNE method (1st row: simulated sources, 2nd row: reconstructed sources).

SCCD is relative small and its median AUC values are high. However, it also reflects the fact that, at a few locations, the performance of VB-SCCD will be significantly reduced. These locations are usually within deep brain structures. The performance of three methods also significantly depends on the number of sources. With the number of sources increases, AUC values decrease.

Figs. 2-4 visualize three examples (with the highest AUC values) in conditions of 5 sources from wMNE, cLORETA, and VB-SCCD, respectively. Note, since they were selected according to the AUC value, these examples from different methods are not from same simulated brain activations. However, by directly viewing these figures and comparing simulated brain activations (1st row) with reconstructed brain activations (2nd row), it is easy to judge which method has the best performance. The reconstructed brain activations were thresholded individually at 20% of the maximal activity in order to remove background for easy visualization

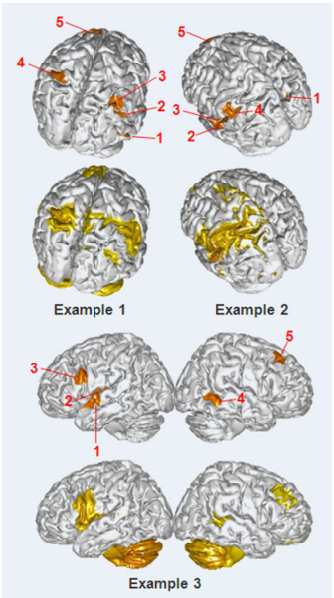

Figure 3 Visualization of three examples with the highest AUC values in the conditions of 5 simultaneous brain activations from the cLORETA method (1st row: simulated sources, 2nd row: reconstructed sources).

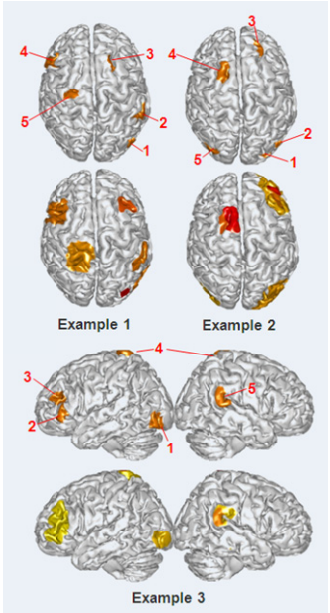

Figure 4 Visualization of three examples with the highest AUC values in the conditions of 5 simultaneous brain activations from the VB-SCCD method (1st row: simulated sources, 2nd row: reconstructed sources).

and comparison. Furthermore, some isolated outlier elements on the CCD model with extremely large values appeared in both results from wMNE and cLORETA. These errors are possibly due to numerical modeling and calculations as discussed in [9], which were manually removed in order to show the valuable information from wMNE and cLORETA. Note that there were no observations of such outlier activity from VB-SCCD.

In Fig. 2, it shows that the wMNE method is able to locate some sources when the brain activation is quite complicated (i.e. 5 sources), meanwhile it has significant problems on false alarms (e.g. example 3) and missing sources (e.g. example 2, source #2 and source #5). The cLORETA method has the similar problems as shown in Fig. 3 (false alarms: all examples; missing sources: example 2, source #5). The performance of VB-SCCD is obviously better than both wMNE and cLORETA. It has no missing sources in these three examples and no significant false alarms away from actually simulated sources. It is also worth to point out there are limitations from the VB-SCCD method too. First, when there are sources close to each other, it is difficult to be distinguished (e.g. example 3, source 2 and source 3). Second, the spatial extent of each reconstructed source seems larger than the simulated extent. Since we only used the simple thresholding technique to remove background activity, these two problems might be partially reduced with more proper thresholding techniques or choosing more suitable thresholds.

IV. Discussion

In the present study, we conducted a simulation study using the Monte Carlo approach, in order to compare the performance of one L1-norm neuroimaging method (i.e. VB-SCCD) and other two L2-norm neuroimaging methods (i.e. wMNE and cLORETA) in reconstructing extended cortical neural electrical activations. From our simulation data, it suggests that the VB-SCCD L1-norm method is able to reconstruct extended cortical sources with the overall high accuracy evaluated by the metric AUC. The VB-SCCD L1-norm method is significantly different from previous reported L1-norm methods [10-13], which are only able to produce and reconstruct focal brain activations even in conditions focal activations are not the case. By directly visualizing reconstructed cortical current densities from wMNE, cLORETA, and VB-SCCD, the distributions from VB-SCCD obviously have significantly less number of false alarms and missing sources. The examples shown in Fig. 4 in reconstructing 5 sources at the same time and the overall strong data in Whisker plots for VB-SCCD all suggest that this new method is able to solve much more complex EEG inverse problems, which cannot be solved by wMNE and cLORETA with satisfactory results.

The difference between wMNE/cLORETA and VB-SCCD seems more significant as shown in Figs. 2-4 than data plotted in Fig. 1. This might suggest the relatively low sensitivity of the AUC metric in evaluating the performance of neuroimaging methods, which might need further research. How we can get the accurate estimation of each source's cortical extent from distributions produced by VB-SCCD (possibly by integrating with thresholding techniques) to obtain more neuroinformatics other than source localizations will be another interesting topic, which can take advantage of inverse solutions from VB-SCCD.

In summary, our newly reported sparse neuroimaging method by exploring the sparseness in the variation map of cortical current densities has a significantly improved performance in reconstructing more complex brain activations (up to five as investigated in the current study). It is promising to have many valuable applications in neuroscience and neurology problems.

References

[1] Nunez PL, 1981. *Electric field of the brain*. London: Oxford University Press.

[2] He B, Lian J, 2005. Electrophysiological Neuroimaging, In He B (Ed): Neural Engineering, Kluwer Academic/Plenum Publishers. 221-262.

[3] Dale AM, Sereno MI, 1993. Improved localization of cortical activity by combining EEG and MEG with MRI cortical surface reconstruction: a linear approach. *J. Cog. Neurosci.* 5, 162-176.

[4] Hämäläinen MS, Ilmoniemi RJ, 1984. Interpreting measured magnetic fields of the brain: estimates of current distributions. Technical Report TKK-F-A559, Helsinki University of Technology.

[5] Jeffs B, Leahy R, Singh M, 1987. An evaluation of methods for neuromagnetic image reconstruction. *IEEE Trans. Biomed. Eng.* 34, 713-723.

[6] Pascual-Marqui RD, Michel CM, Lehmann D, 1994. Low resolution electromagnetic tomography: a new method for localizating electrical activity in the brain. *Int. J. Psychophysiol.* 18, 49-65.

[7] Liu AK, Belliveau JW, Dale AM, 1998. Spatiotemporal imaging of human brain activity using fMRI constrained MEG data: Monte Carlo simulations. *Proc. Natl. Acad. Sci. USA.* 95, 8945-8950.

[8] He B, Yao D, Lian J, Wu D, 2002. An equivalent current source model and Laplacian weighted minimum norm current estimates of brain electrical activity. *IEEE Trans. Biomed. Eng.* 49, 277-288.

[9] Ding L, 2009. Reconstructing Cortical Current Density by Exploring Sparseness in the Transform Domain. *Physics in Medicine and Biology*, in press.

[10] Matsuura K, Okabe Y, 1995. Selective minimum-norm solution of the biomagnetic inverse problem. *IEEE Trans. Biomed. Eng.* 42, 608-615.

[11] Wagner M, Wischmann HA, Fuchs M, Kohler T, Drenckhahn R, 1998. Current density reconstruction using the L1 norm. Advances in Biomagnetism Research: Biomag96, Springer-Verlag, New York. 393-396.

[12] Uutela K, Hamalainen M, Somersalo E, 1999. Visualization of Magnetoencephalographic Data Using Minimum Current Estimates. *NeuroImage*. 10, 173-180.

[13] Ding L, He B, 2007. Sparse source imaging in EEG with accurate field modeling. *Human brain mapping*. [Epub ahead of print], Sep. 25.

[14] Wagner M, Fuchs M, Wischmann HA, Drenckhahn R, Köhler T, 1996. Smooth reconstruction of cortical sources from EEG or MEG recordings. *NeuroImage* 3:S168.

[15] Grova C, Daunizeau J, Lina JM, Benar CG, Benali H, Gotman J, 2006. Evaluation of EEG localization methods using realistic simulations of interictal spikes. *NeuroImage* 29:734-753.

[16] Liu AK, Dale AM, Belliveau JW, 2002. Monte Carlo Simulation Studies of EEG and MEG Localization Accuracy. *Hum Brain Mapp* 16:47-62.

[17] Morozov AV, 1966. On the solution of functional equations by the method of regularization. *Soviet. Math. Dokl*. 7, 414-417.

[18] Nemirovski A, Ben Tal A, 2001. Lectures on Modern Convex Optimization. Analysis, Algorithms and Engineering Application, SIAM.

[19] Sturm JS, 2001. Using SeDuMi 1.02, a Matlab toolbox for optimization over symmetric cones. Netherlands: Tilburg University, Department of Econometrics.

[20] Zhang Y, van Drongelen W, He B, 2006. Estimation of *in vivo* human brain-to-skull conductivity ratio in humans. *Applied Physics Letters.* 89, 223903.